Journal of ELECTRONIC MATERIALS, Vol. 43, No. 9, 2014
DOI: 10.1007/s11664-014-3245-8

Enhancement of Processability and Electrical Resistance by Use of Ag-Based Composite Inks Containing Ultrafine SAC305 Alloy Nanoparticles

YONG MOO SHIN,[1] HYUN-JIN KIM,[2] SEOK PIL JANG,[2,3] and JONG-HYUN LEE[1,4]

1.—Department of Materials Science and Engineering, Seoul National University of Science and Technology, 232 Gongneung-ro, Nowon-gu, Seoul 139-743, Republic of Korea. 2.—School of Aerospace and Mechanical Engineering, Korea Aerospace University, 76 Hanggongdaehang-ro, Deogyang-gu, Goyang-si, Gyeonggi-do 412-791, Republic of Korea. 3.—e-mail: spjang@kau.ac.kr. 4.—e-mail: pljh@snut.ac.kr

We propose use of Ag/Sn-3.0 (wt.%) Ag-0.5 Cu (SAC305) composite ink to reduce sintering temperature, sintering time, and material costs. The SAC305 nanoparticle (NP) surfaces were not capped by any stabilizers, which are detrimental to the resistivity of the sintered tracks. Compared with commercial pure Ag ink, use of Ag/3.2 (vol.%) SAC305 composite ink containing ultrafine SAC305 NPs resulted in outstandingly enhanced processability, enabling faster sintering at low temperatures. The average sheet resistance of composite ink samples sintered for 25 min at 170°C was as low as 0.011 Ω/□, comparable with that of a pure Ag sample sintered for over 30 min at 220°C. The morphology and the differential scanning calorimetry curves enabled explanation of the changes in the sintering behavior and sheet resistance. The Ag/SAC305 clusters in the composite ink sintered at 170°C grew, on average, to ~201.1–226.1 nm as a result of faster local liquid-phase sintering, and most of the Ag particles were mutually linked, dramatically changing the microstructure.

Key words: Composite ink, Sn-3.0Ag-0.5Cu (SAC305) nanoparticle, low-temperature sintering, liquid-phase sintering, sheet resistance

INTRODUCTION

Compared with conventional methods used for photolithographic production of conducting tracks, inkjet printing is simpler, more efficient, and more cost effective[1–6]; hence, it should emerge as the principal method for forming conducting tracks for printed electronics.[7,8] Silver has been extensively studied for use as a crucial material in printing inks, because of its outstanding electrical characteristics and oxidation resistance, and Ag-based ink products are already available commercially.[9]

However, Ag-based inks require high sintering temperatures and long sintering times and the raw materials for producing Ag-based inks are expensive.[5,9–11] Although Ag-based inks must be sintered for only 10 min to achieve a sintered microstructure, they must be sintered in the range 200–300°C to produce highly conducting tracks.[10,11] Further, the lower the sintering temperature, the longer the inks must be sintered to achieve critical conductivity.[10] Use of an Ag–Cu composite ink has previously been suggested to reduce the cost of producing Ag-based inks, and its processability and physical properties have been studied.[12] The electrical resistivity of the optimized Ag:3Cu composite track sintered at 200°C under vacuum (10^{-3} Torr) reached ~23.6 $\mu\Omega$ cm[12]; however, low sintering temperatures and short sintering times could not be achieved, owing to the intrinsically high melting points of Cu and Ag. Reducing the sintering

(Received November 21, 2013; accepted May 9, 2014; published online June 6, 2014)

temperature enables more transparent, less expensive, less thermally stable plastic substrates to be used and enables the desired substrate to be chosen from among a broader range of readily available flexible substrates. Moreover, shortening the sintering time eliminates the need to install a long-sintering furnace.

To reduce sintering temperature, shorten sintering time, and slightly lower the cost of producing the inks, we examined the processability of Ag/Sn-3.0 (wt.%) Ag-0.5 Cu (SAC305) composite printing inks and studied the electrical properties of sintered tracks. As already reported, the melting point (217°C) of bulk SAC305 alloy nanoparticles (NPs) decreases substantially, because of the Gibbs–Thomson effect, when the particles are smaller than 20–30 nm.[13,14] Thus, a conducting network between the Ag NPs could be formed by liquid-phase sintering at a relatively low temperature, depending on the size of the SAC305 NPs, if the SAC305 NPs are inserted between the Ag NPs. In other words, the SAC305 NPs could act as a liquid binder, producing a conducting network between the Ag NPs. SAC305-NP-induced reduced-melting-point liquid-phase sintering could simultaneously lower the sintering temperature and shorten the sintering time.

EXPERIMENTAL

To prepare the composite inks, a specific amount of SAC305-NP-containing benzyl alcohol solution containing a trace amount of flux was decanted into pure Ag ink (DGP 40TE-20C; Advanced Nano Products) and the resulting solution was mixed by use of a homogenizer (Pro-200; Pro Scientific). The resulting solution was then mixed under ambient conditions for 30 s and then for another 30 s in a sonication bath. Energy-dispersive x-ray spectrometry (EDS; Noran System Six; Thermo Electron) was used to analyze the cross-sections of the subsequently sintered ink layers to determine the compositions of the composite inks.

A micropipette (Research Plus 3120 000.046; Eppendorf) was used to drop 50 μL of the prepared composite inks on to 1 cm × 1 cm Si wafers. The ink-coated wafers were sintered in air in the range 140–170°C for 10–30 min. Differential scanning calorimetry (DSC; Q20; TA instruments) was used with ~10-mg SAC305 solution samples under N_2 (flow rate 50 mL/min) for quantitative analysis of the melting behavior of the SAC305 NPs with increasing temperature.

The microstructures of the sintered layers were observed by use of field-emission scanning electron microscopy (FE-SEM; Inspect F50; FEI). The room-temperature sheet resistance of the sintered layers was measured by use of a four-point probe linked to a Semiconductor Parameter Analyzer (SPA; 4155C; Agilent Technologies). The total distance between the probes, set at 1-mm intervals, was 3 mm.

RESULTS AND DISCUSSION

Pure Ag ink was purchased and used as the base ink to produce the Ag/SAC305 composite inks. SAC305 NPs were fabricated at Able Metal. The size and morphology of the Ag and SAC305 NPs were characterized by use of high-resolution transmission electron microscopy (HR-TEM; Tecnai 20; FEI). The diameter of the Ag NPs in the Ag ink ranged from 16.2 nm to 99.0 nm, and the average diameter was ~42.8 nm ($\sigma \leq 28.1\%$, standard deviation), as shown in Fig. 1a. Figure 1b shows the HR-TEM image of the SAC305 NPs produced in-house and preserved in benzyl alcohol to prevent oxidation. The surfaces of the SAC305 NPs were not capped by stabilizers. The NPs were either spherical or slightly ellipsoidal with relatively uniform size distribution. The diameters of the SAC305 NPs ranged from 4.4 nm to 14.5 nm, and the average diameter was ~8.2 nm ($\sigma \leq 22.4\%$). The average melting

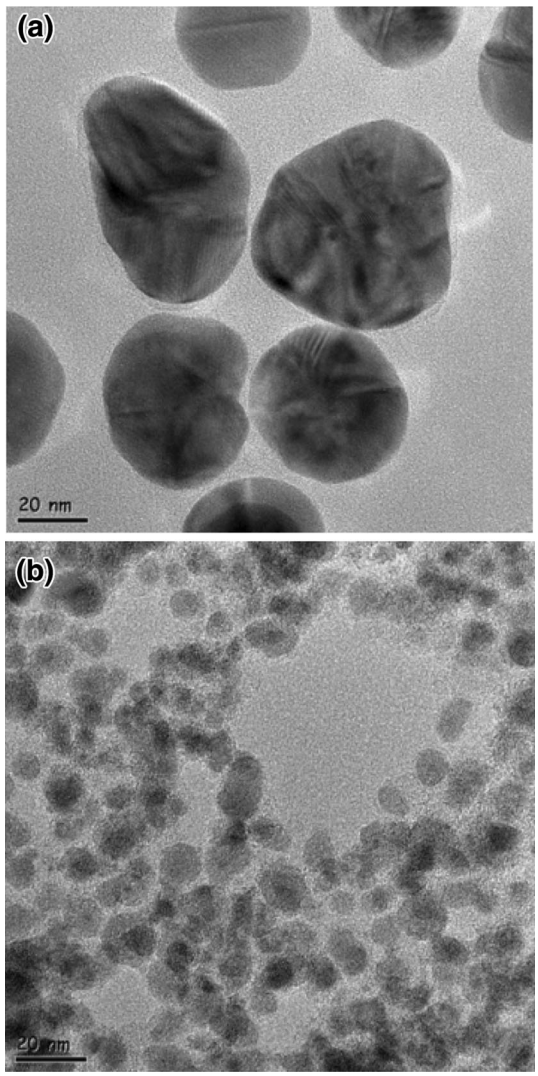

Fig. 1. HR-TEM image of (a) commercial pure Ag ink and (b) as-prepared SAC305 NPs used to fabricate composite inks.

point of the NPs was estimated to be ~140°C, according to the calculation of Gao et al.[14] During sintering, the SAC305 NPs were expected to serve as a liquid binder during fabrication of the conducting track, according to the sintering mechanism predicted for the Ag/SAC305 composite ink. Thus, the electrical resistivity of the track was expected to increase when we used a capping agent such as polyvinylpyrrolidone (PVP) to encapsulate the SAC305 NPs.[15] To avoid this effect, we added uncapped SAC305 NPs to the prepared composite inks.

Figure 2 shows the room-temperature sheet resistance of ~3.5-μm-thick layers of commercial pure Ag ink sintered at different temperatures and for different times. The resistance of all samples decreased with increasing sintering temperature and time. However, no significant reduction in sheet resistance was observed for the sample sintered at 180°C, even after 60 min. Increasing the sintering temperature significantly reduced the sheet resistance. The sheet resistance of the sample sintered at 220°C for 20 min nearly stabilized to 0.013 Ω/□ ($\sigma \leq 2.4\%$) whereas that of the sample sintered at 200°C only stabilized after 30 min. The sample sintered at 220°C for 60 min had the lowest sheet resistance, 0.008 Ω/□ ($\sigma \leq 41.5\%$).

Figure 3 shows the sheet resistance of Ag/3.2 (vol.%) SAC305 composite ink layers sintered in the range 150–170°C, approximately the depressed melting temperature of SAC305 NPs, for different lengths of time. Although the sheet resistance for all the samples decreased with increasing sintering temperature and time, increasing the sintering temperature significantly reduced the sheet resistance, despite sintering of the samples at relatively low temperatures. The samples sintered at 150°C and 160°C had lower sheet resistance, evidently proportional to the holding time, whereas the layer sintered at 150°C had high resistivity even after 30 min. The behavior of the sample sintered at 170°C was most surprising: its sheet resistance decreased to 0.019 Ω/□ ($\sigma \leq 25.1\%$) after only 10 min and further decreased to 0.014 Ω/□ ($\sigma \leq 13.4\%$) after 15 min. The average sheet resistance measured for samples sintered for 25 min was as low as 0.011 Ω/□ ($\sigma \leq 17.9\%$), similar to that measured for the pure Ag sample sintered for over 30 min at 220°C, implying that the sintering temperature required to achieve sheet resistance similar to that for pure Ag ink annealed at 220°C was significantly reduced, and indicating that sheet resistance was significantly improved compared with previous Ag-based inks.[10,11]

The ink microstructures were analyzed to elucidate whether the composite inks could effectively and quickly stabilize the electrical resistance with lower energy consumption. Figure 4 shows representative surface microstructures of the pure Ag ink layers sintered at different temperatures for different times. The microstructures in all the layers indicated that the Ag NPs tended to grow by agglomeration and coalescence with increasing sintering temperature and time, thereby eliminating the interfaces and voids between the Ag NPs and accounting for the reduced sheet resistance shown in Fig. 2. Maximum particle diameters for layers sintered for 10 min at 180°C, 200°C, and 220°C were ~164.2 nm, ~277.4 nm, and ~441.0 nm, respectively.

Representative surface microstructures of Ag/3.2 SAC305 composite ink layers sintered at different temperatures for different times are shown in Fig. 5. The microstructures of all the layers indicate that the Ag/SAC305 clusters, specifically, grew by faster agglomeration and coalescence with increasing sintering temperature. The microstructure of the sample sintered at 150°C changed substantially with increasing holding time. The microstructure of the sample annealed for 15 min (Fig. 5a) contained

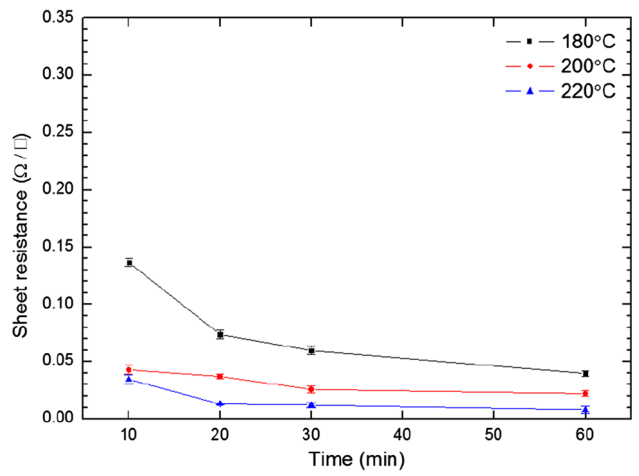

Fig. 2. Sheet resistance of sintered pure Ag ink layers plotted as functions of time for different sintering temperatures.

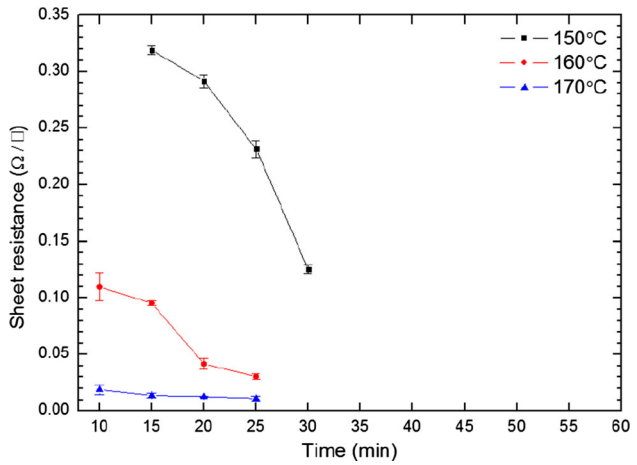

Fig. 3. Sheet resistance of sintered Ag/3.2 SAC305 composite ink layers plotted as functions of time for different sintering temperatures.

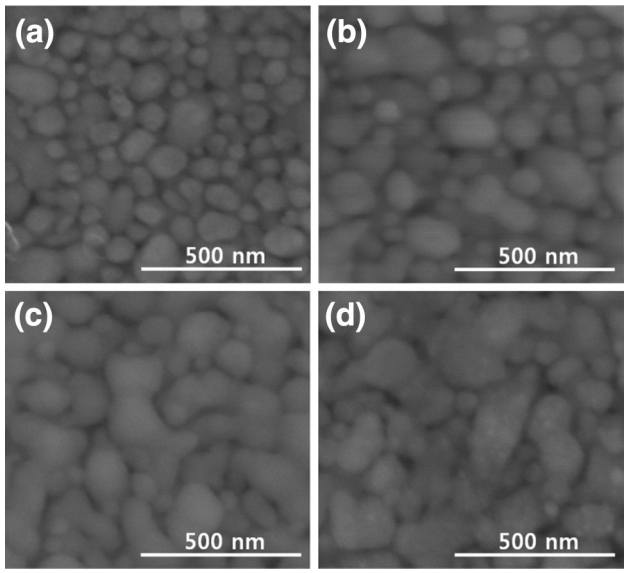

Fig. 4. SEM images of pure Ag layers sintered at different temperatures and for different times: (a) 10 min at 180°C (average particle diameter: 130.0 nm, $\sigma \leq 23.0\%$), (b) 60 min at 180°C (177.0 nm, $\sigma \leq 20.0\%$), (c) 10 min at 200°C (192.3 nm, $\sigma \leq 24.2\%$), and (d) 10 min at 220°C (224.5 nm, $\sigma \leq 26.3\%$).

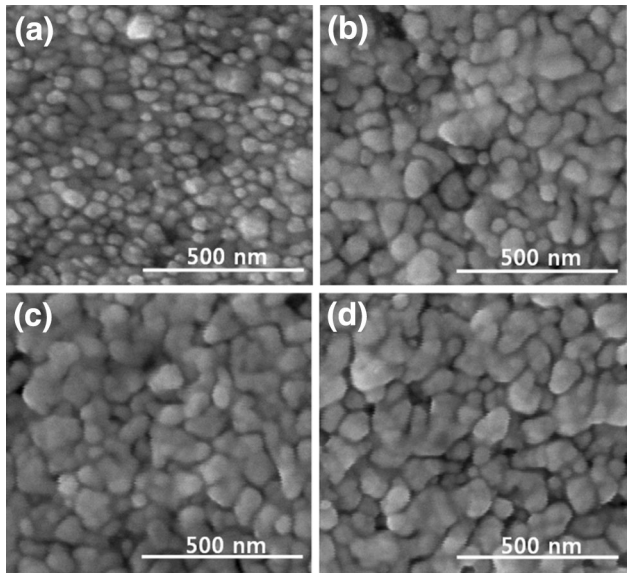

Fig. 5. SEM images of Ag/3.2 SAC305 layers sintered for (a) 15 min at 150°C (average particle diameter: 52.2 nm, $\sigma \leq 37.5\%$), (b) 30 min at 150°C (116.9 nm, $\sigma \leq 52.6\%$), (c) 10 min at 170°C (201.1 nm, $\sigma \leq 39.2\%$), and (d) 25 min at 170°C (221.3 nm, $\sigma \leq 19.2\%$).

Ag particles and SAC305 NPs a few nanometers in diameter, and only a few Ag particles had agglomerated and coarsened. However, notable agglomeration and coarsening of the Ag particles were observed for the sample sintered for 30 min (Fig. 5b). As a result, average particle diameters of 52.2 ($\sigma \leq 37.5\%$) and 116.9 nm ($\sigma \leq 52.6\%$) were observed for layers sintered for 15 and 30 min, respectively, at 150°C. The sample sintered at 170°C for 10 min (Fig. 5c) had a more agglomerated, coarsened microstructure and contained few isolated particles. Numerous SAC305 NPs of slightly different sizes melted at high sintering temperatures. These results clearly account for the excellent resistivity shown in Fig. 3. Particle agglomeration and coalescence were marginally accelerated when the holding time was increased to 25 min (Fig. 5d), corresponding to the slightly decreased resistivity shown in Fig. 3.

Eliminating the interfaces and voids between the Ag particles accounts for the drastically reduced resistivity depicted in Fig. 3. Melting SAC305 NPs may have induced particle agglomeration and coalescence, which, in turn, induced drastic changes of the microstructure. SAC305 NPs, which, owing to the Gibbs–Thomson effect, melt at a temperature lower than that at which bulk SAC305 melts, may wet the surface of the Ag particles. Further, the surface tension of the molten SAC305 would cause the Ag particles to gravitate toward each another, eventually facilitating particle agglomeration and coalescence. However, the molten SAC305 wetting the Ag particle surfaces may resolidify, owing to an increased radius of curvature.[16] Thus, the melting behavior which results from the SAC305 NP-depressed melting point may lead to local and transient liquid-phase sintering in the composite inks. The marginally accelerated change in the microstructure shown in Fig. 5d implies that the post-resolidification solid-state sintering of molten SAC305 at 170°C is tardy.

The microstructures formed at 150°C depended on the holding time, because of the time required to evaporate the high-boiling-point solvent (benzyl alcohol) in the composite inks. It is expected that heating the samples for 15 min at 150°C almost completely evaporates the benzyl alcohol; therefore, the molten SAC305 NPs cannot initially wet the Ag particles, as shown in Fig. 5a, because any remaining solvent hinders wetting. Hence, optimizing the solvent can enhance the wetting behavior of molten SAC305 NPs. Some ultrafine SAC305 NPs whose melting points are below 150°C, on the other hand, would effectively wet the Ag particles and act as a liquid binder when the solvent was completely evaporated after a sufficiently long holding time, as shown in Fig. 5b. However, some isolated Ag particles still remained because some SAC305 NPs added at 150°C did not melt, thus accounting for the inadequate resistivity shown in Fig. 3. Increasing the temperature to 170°C is expected to increase the rate of evaporation of the benzyl alcohol.

Figure 6 shows the DSC curves plotted for increasing holding time at 140°C or 160°C for the SAC305 NP solution used to fabricate the composite inks. The samples were dynamically heated at 30°/min to 140°C and 160°C in 3.66 min and 4.33 min, respectively, and were subsequently heated isothermally. The solvent (benzyl alcohol) progressively

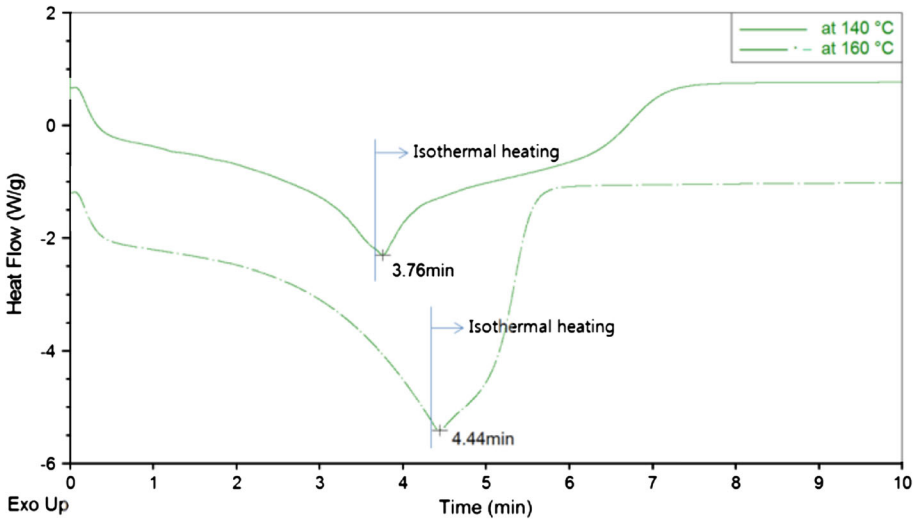

Fig. 6. DSC curves for SAC305-NP-containing solution plotted as functions of holding time at 140°C and 160°C.

evaporated, resulting in endothermic heat flow during the early stage of heating. The slope of the endothermic peak steepened increasingly until isothermal heating began. Very few additional endothermic heat flows were observed after the initial isothermal heating. Although similar amounts of SAC305 solutions were used in both experiments, and the solvents were completely evaporated, the total areas under the endothermic peaks were markedly different, indicating that more SAC305 NPs had melted at the higher temperature (160°C) and that the number of SAC305 NPs that had melted at 140°C might be negligible. In other words, the wider area under the endothermic peak measured at 160°C suggests that the SAC305 NPs had melted more effectively at that temperature, which is a reasonable inference considering that slightly changing the SAC305 NP size significantly altered the melting point.[13,14] Further, this observation explains the temperature-dependent and time-dependent sintering characteristics of the composite ink shown in Fig. 5.

Figure 7 shows the sheet resistance of Ag/6.4 SAC305 composite ink layers sintered in the range 140–170°C, increasing in 10° increments, for 30–15 min, decreasing in 5-min increments because the benzyl alcohol slowly evaporated. Therefore, the samples were sintered at 140°C, 150°C, 160°C, and 170°C for 30 min, 25 min, 20 min, and 15 min, respectively. The sheet resistance decreased steeply with increasing sintering temperature from 140°C to 160°C. However, the sheet resistance of the sample sintered at 170°C decreased only slightly, to 0.018 Ω/□ ($\sigma \leq 26.2\%$), which was slightly higher than that of the Ag/3.2 SAC305 layer formed under identical sintering conditions.

Representative surface microstructures of Ag/6.4 SAC305 composite ink layers sintered in the range 140–170°C for different times are shown in Fig. 8. The connectivity between the Ag particles increased

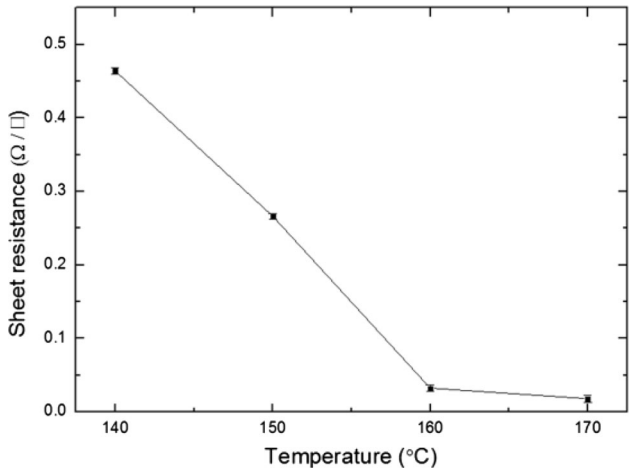

Fig. 7. Sheet resistance of sintered Ag/6.4 SAC305 composite ink layers plotted as a function of temperature. Samples were sintered for 15–30 min, depending on sintering temperature.

substantially in proportion to sintering temperature. Hardly any liquid-phase sintering was observed for the sample sintered at 140°C (Fig. 8a). However, enhanced connectivity was observed for that sintered at 160°C (Fig. 8c). Although the holding time was shortened with increasing temperature, higher sintering temperatures effectively evaporated the solvent and melted more SAC305 NPs. The sample heated at 170°C (Fig. 8d), which was expected to be the temperature at which the most SAC305 NPs would melt, had hardly any voids, because the microstructure of the sintered particles was more uniform than that of samples heated at 150°C and 160°C (Figs. 8b and c). However, the sheet resistance (0.018 Ω/□) of the Ag/6.4 SAC305 composite ink sample (Fig. 8d) sintered for 15 min at 170°C was slightly higher than that (0.014 Ω/□) of the identically sintered Ag/3.2 SAC305 sample. Moreover, the sheet resistance of

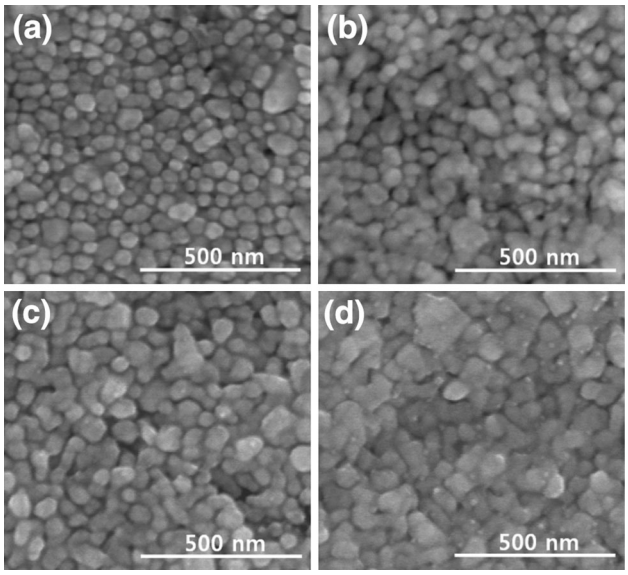

Fig. 8. SEM images of Ag/6.4 SAC305 layers sintered for (a) 30 min at 140°C (average particle diameter: 52.1 nm, $\sigma \leq 34.5\%$), (b) 25 min at 150°C (127.0 nm, $\sigma \leq 49.0\%$), (c) 20 min at 160°C (198.2 nm, $\sigma \leq 28.9\%$), and (d) 15 min at 170°C (226.1 nm, $\sigma \leq 27.7\%$).

the prepared Ag/14.3 SAC305 sample reached ~0.154 Ω/□. The total void volume, calculated theoretically from the density of randomly close-packed spheres, is 26%, higher than 6.4% or 14.3%. Hence, the sheet resistance should decrease consistently to 26% with increasing amounts of SAC305 NPs. Nevertheless, the sheet resistance of the sintered layers increased with increasing SAC305 NP content, which can be explained by the amount of actual linkage between the Ag NPs as a result of SAC305 wetting during heating. Aggregation of the added SAC305 NPs can hinder the sintering of close-packed spheres and transient liquid-phase sintering, as discussed below.

Figure 9 shows schematic diagrams illustrating the wetting behavior of the composite inks on the basis of the transient liquid-phase sintering characteristics of nano-Ag/ultrafine nano-SAC305 inks. The Ag NPs can be physically and electrically linked as a result of SAC305 melting and wetting during heating, when the SAC305 NPs are ideally in direct contact with the Ag NPs (Fig. 9a). However, the Ag and SAC305 NPs (Fig. 9b) cannot be linked if there is space between them at low temperatures, because SAC305 NPs grow by agglomeration, instantly increasing the melting temperature, when they are not in contact with the Ag NPs. Vertically aligned SAC305 NPs require a more detailed discussion. The large-SAC305-NP/Ag-NP interface cannot be linked whereas small-SAC305-NP/Ag-NP interfaces can be linked when small and large SAC305 NPs are vertically stacked between two Ag NPs (Fig. 9c; the size of neighboring SAC305 NPs always differs). Thus, an effective electrical path cannot usually be generated. The four interfaces can be linked where

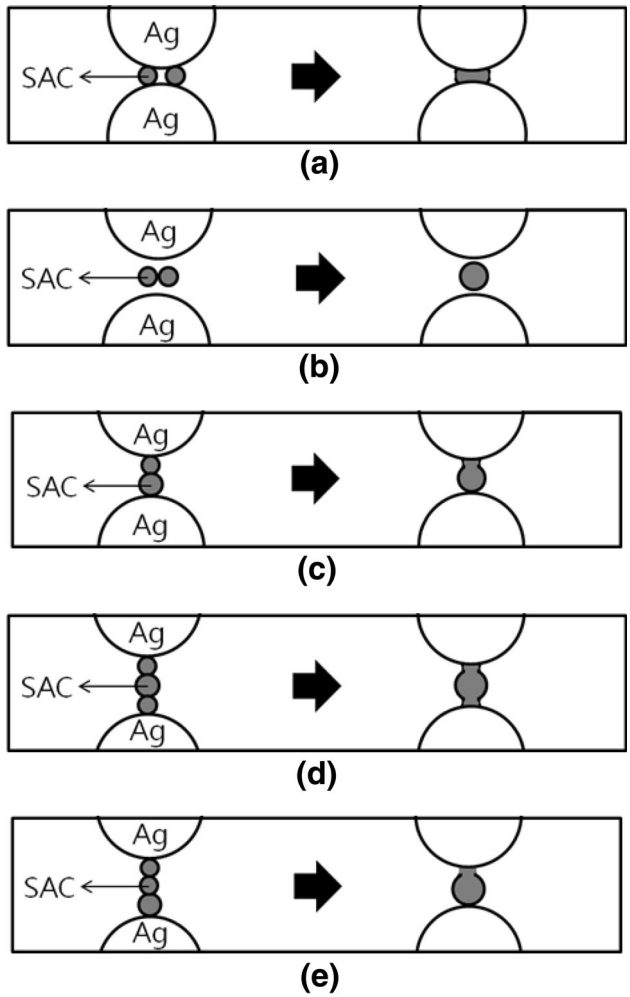

Fig. 9. Schematic diagrams illustrating a case study of the transient liquid-phase sintering characteristics of Ag/SAC305 composite inks. Particles are vertically aligned in the order: (a) Ag/SAC305/Ag, (b) Ag/space/SAC305/space/Ag, (c) Ag/small SAC305/large SAC305/Ag, (d) Ag/small SAC305/large SAC305/small SAC305/Ag, and (e) Ag/small SAC305/small SAC305/large SAC305/Ag.

small/large/small SAC305 NPs align vertically (Fig. 9d). However, the four interfaces cannot be linked when the large SAC NP is in direct contact with the Ag NP (Fig. 9e), which might happen often. On the basis of similar reasoning, we postulate that forming a complete link would be highly improbable where more than four SAC305 NPs are vertically aligned. In other words, a complete link can form only when the particles are arranged in a regular sequence as follows: Ag NP/small SAC305 NP/large SAC305 NP/small SAC305 NP/large SAC305 NP…/small SAC305 NP/Ag NP. Thus, the wetting behavior of the composite inks can account for the increased electrical resistivity with increasing amount of added, imperfectly separated, SAC NPs (i.e., the aggregated as-prepared SAC305 NPs shown in Fig. 1b). In comparison with the Ag/3.2 SAC305 samples (Fig. 5c, d) sintered for 10 min and 25 min at 170°C, a substantially enhanced average particle diameter was not observed for the Ag/6.4

SAC305 sample (Fig. 8d) sintered for 15 min at 170°C; this is further indirect evidence of such wetting behavior.

CONCLUSIONS

Compared with commercial pure Ag ink, the processability of Ag/3.2 SAC305 composite ink containing ultrafine SAC305 NPs was outstandingly enhanced and the ink could be rapidly sintered even at low temperatures. The average sheet resistance measured for Ag/3.2 SAC305 composite ink samples sintered for 25 min at 170°C was as low as 0.011 Ω/□, similar to that measured for the pure Ag sample sintered for over 30 min at 220°C. The morphology and the DSC curves explained the marked changes in sheet resistance. The Ag particles in the composite ink grew, on average, to 224.5 nm as a result of rapid local liquid-phase sintering at 170°C, linking most of the Ag particles and thus dramatically changing the microstructure. Because these results provide a real solution to the process delays which occur during use of conventional Ag-based inks, Ag/SAC305 composite inks are a new model for production of conducting metal-based ink materials.

ACKNOWLEDGEMENTS

This work was supported by the National Research Foundation of Korea funded by the Ministry of Education, Science, and Technology (2011-0009088). The authors thank Able Metal Co., Ltd (http://www.ablemetal.co.kr) for the SAC305 NPs and the Korean Basic Science Institute (Seoul) for the TEM images.

REFERENCES

1. H. Sirringhaus, T. Kawase, R.H. Friend, T. Shimoa, M. Inbasekaran, W. Wu, and E.P. Woo, *Science* 290, 2123 (2000).
2. D. Huang, F. Liao, S. Molesa, D. Redinger, and V. Subramanian, *J. Electron. Soc.* 150, G412 (2003).
3. Q. Cao, H.-S. Kim, N. Pimparkar, J.P. Kulkarni, C. Wang, M. Shim, K. Roy, M.A.A. Alam, and J.A. Rogers, *Nature* 454, 495 (2008).
4. E. Fisslthaler, S. Sax, U. Scherf, G. Mauthner, E. Moderegger, K. Landfester, and E.J.W. List, *Appl. Phys. Lett.* 92, 183305 (2008).
5. J. Perelaer, M. Klokkenburg, C.E. Hendriks, and U.S. Schubert, *Adv. Mater.* 21, 4830 (2009).
6. J.D. Kim, J.S. Choi, B.S. Kim, Y.C. Choi, and Y.W. Cho, *Polymer* 51, 2147 (2010).
7. Y. Li, Y. Wu, and B.S. Ong, *J. Am. Chem. Soc.* 127, 3266 (2005).
8. K.J. Lee, B.H. Jun, T.H. Kim, and J. Joung, *Nonotechnology* 17, 2424 (2006).
9. S. Joo and D.F. Baldwin, *Proceedings of 57th ECTC* (EIA/IEEE, 2007), pp. 219–226.
10. J. Perelaer, A.W.M. de Laat, C.E. Hendriks, and U.S. Schubert, *J. Mater. Chem.* 18, 3209 (2008).
11. S. Magdassi, M. Grouchko, O. Berezin, and A. Kamyshny, *ACS Nano* 4, 1943 (2010).
12. K. Woo, D. Kim, J.S. Kim, S. Lim, and J. Moon, *Langmuir* 25, 429 (2009).
13. C.D. Zou, Y.L. Gao, B. Yang, X.Z. Xia, Q.J. Zhai, C. Andersson, and J. Liu, *J. Electron. Mater.* 38, 351 (2009).
14. Y. Gao, C. Zou, B. Yang, Q. Zhai, J. Liu, E. Zhuravlev, and C. Schick, *J. Alloys Compd.* 484, 777 (2009).
15. Y.H. Jo, I. Jung, C.S. Choi, I. Kim, and H.M. Lee, *Nanotechnology* 22, 225701 (2011).
16. S–.S. Chee and J.-H. Lee, *Appl. Mech. Mater.* 249–250, 939 (2013).